symmetry

IMPACT FACTOR 2.2

CITESCORE 5.4

Article

Lepton Flavour Universality in Rare B Decays

Paula Álvarez Cartelle and Richard Morgan Williams

Special Issue

Symmetries and Anomalies in Flavour Physics

Edited by

Dr. Stefania Ricciardi, Dr. Thomas Blake and Dr. Farvah Nazila Mahmoudi

MDPI

https://doi.org/10.3390/sym16070822

symmetry

MDPI

Article

Lepton Flavour Universality in Rare B Decays

Paula Álvarez Cartelle *,† **and Richard Morgan Williams** *,†

Cavendish Laboratory, University of Cambridge, Cambridge CB3 0HE, UK
* Correspondence: paula.alvarez@cern.ch (P.Á.C.); richard.morgan.williams@cern.ch (R.M.W.)
† These authors contributed equally to this work.

Abstract: Tests of lepton flavour universality in rare decays of b hadrons mediated by flavour-changing neutral-current transitions constitute sensitive probes for physics beyond the standard model. In recent years, such tests have become increasingly precise and have attracted significant theoretical and experimental attention. In this article, we review the status of searches for lepton flavour universality violations in these processes and discuss prospects for future measurements at various facilities.

Keywords: flavour physics; rare decays; flavour anomalies; lepton flavour universality

check for updates

Citation: Álvarez Cartelle, P.; Williams, R.M. Lepton Flavour Universality in Rare B Decays. *Symmetry* **2024**, *16*, 822. https://doi.org/10.3390/sym16070822

Academic Editor: Francesco Renga

Received: 15 May 2024
Revised: 4 June 2024
Accepted: 7 June 2024
Published: 30 June 2024

1. Introduction

In the standard model (SM), the couplings of the gauge bosons to the leptons are independent of the lepton flavour. As a consequence, the properties of leptonic and semileptonic decays, differing only in the flavour of the leptons produced, are expected to be identical—up to the effects related to the lepton mass. This so-called lepton flavour universality (LFU) can, however, be violated in many new physics (NP) scenarios, making searches for violations of universality particularly effective as probes for physics beyond the SM.

Lepton flavour universality has been thoroughly tested in the past. It has been verified directly in the comparison of decay widths of the W and Z bosons to different families of leptons and it has been established in the study of multiple decays of leptons and hadrons [1]. A compilation of some of these tests is shown in Figure 1. The variety of the tests performed to date reflect the complementarity between different measurements in the search for physics beyond the SM, as different kinds of NP models could modify the leptonic couplings in specific decays while respecting other LFU constraints [2–4]. The exploration of LFU in all of these sectors is, therefore, crucial to maximise the potential of an NP discovery.

The decays of b hadrons involving the flavour-changing neutral–current $b \to s(d)\ell^+\ell^-$ transition, where ℓ represents any lepton, can also be used as a particularly powerful test of lepton flavour universality. These processes are suppressed in the SM where they can only proceed through electroweak loop diagrams. Beyond the SM, these *rare decays* are sensitive to virtual contributions from new heavy particles and can probe mass scales far beyond what is accessible to direct production at current colliders. One of the lowest-level diagrams for the $b \to s(d)\ell^+\ell^-$ decay in the SM is shown in Figure 2, together with an example of a tree-level process that could result in a measurable effect.

In recent years, measurements of branching ratios [5–8] and angular observables [9–19] in several of these $b \to s\ell^+\ell^-$ decays have shown tensions with SM predictions. A model-independent interpretation of all of these measurements in the context of an effective theory points to a modification of the $b \to s$ coupling with a significance of around 4σ [20–23]. However, theoretical predictions for exclusive $b \to s\ell^+\ell^-$ decays are complicated by the non-perturbative nature of QCD and the uncertainties on the predictions needed for such interpretations are subject to considerable debate [24–27]. In contrast, lepton-universality

tests in these decays can be precisely predicted in the SM, as the hadronic effects are expected to be identical in decays involving different flavours of leptons. Consequently, any sign of lepton flavour non-universality here would be a direct sign for physics beyond the SM.

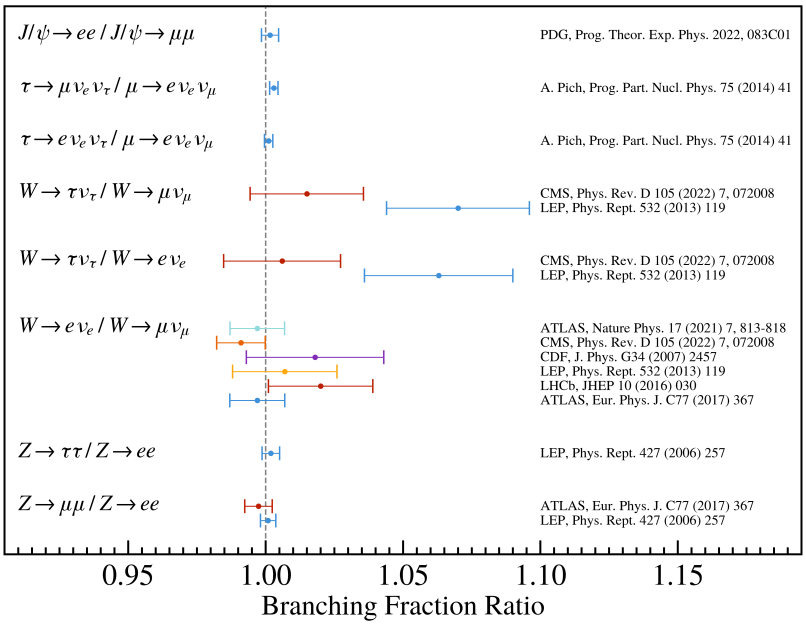

Figure 1. Summary of LFU measurements in different decays [1,28–35].

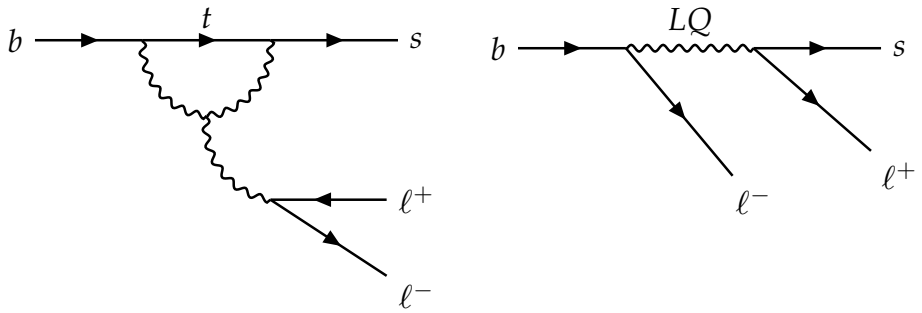

Figure 2. Contributions to the $b \to s\ell\ell$ decay: (**left**) the lowest order SM loop process and (**right**) a hypothetical tree-level NP contribution from a leptoquark (LQ).

A summary of the most recent searches for LFU violation in rare b-hadron decays is presented in this article, focusing on comparisons between electrons and muons. Additional tests of LFU are also performed in the more abundant decays of b hadrons mediated by the charged-current $b \to c\ell^-\bar{\nu}_\ell$ transition. Persistent tension between the couplings of τ and μ leptons has been observed in $B \to D^{(*)}\ell^+\nu_\ell$ decays [36–45] (The inclusion of charge-conjugate processes is implied throughout this document). Different models trying to explain these observations would predict significant effects in the rare decays of b-mesons, particularly in processes mediated by the $b \to s\tau^+\tau^-$ transition [46–48]. Because of the challenging experimental reconstruction of τ leptons, no such transitions have been observed to date. A short discussion on the status of $b \to s\tau^+\tau^-$ searches and prospects in current and future experiments is also included.

2. Experimental Challenge

Branching ratios of $b \to s\ell^+\ell^-$ decays have been measured to be of $\mathcal{O}(10^{-6})$ or smaller. Therefore, to achieve the required precision for LFU tests in such processes, large data samples of b hadrons are required. The small rates for these rare decays also call for efficient

discrimination against different kinds of background processes. Currently, these processes are mainly studied by two active experiments: the Belle II experiment [49] operating at the SuperKEKB B-factory and the LHCb experiment [50] at the LHC. The different production mechanisms of b hadrons in these two environments drastically influence the design of the detectors, as shown in Figure 3. Other general-purpose detectors, such as ATLAS [51] and CMS [52], also study the properties of b hadrons but they are usually limited by the bandwidth dedicated to this part of the physics program.

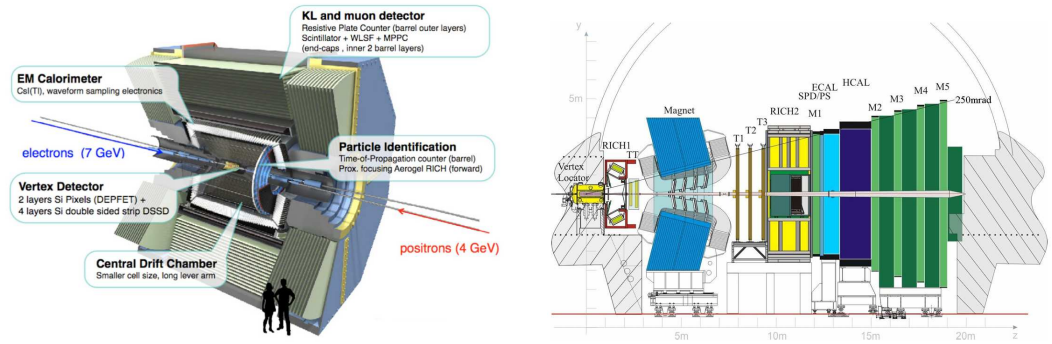

Figure 3. Schematic view of the Belle II [49] (**left**) and LHCb [50] (**right**) experiments.

At the B-factories, electrons and positrons collide at a centre-of-mass energy corresponding to the $\Upsilon(4S)$ resonance, which promptly decays into a pair of quantum correlated b-mesons (B^+B^- or $B^0\overline{B^0}$). This mechanism provides very clean samples with a low amount of incoherent background. In addition, the full reconstruction of one of the B-mesons produced in the $\Upsilon(4S) \to B\bar{B}$ decay (B_{tag}), can be used to infer information regarding the other B-meson (B_{sig}) on which the search for the desired signal can be performed. This approach is particularly useful for decays with missing energy. As the $\Upsilon(4S)$ resonance is produced with a small total momentum, detectors such as Belle II are slightly asymmetric and cover most of the solid angle around the interaction point.

In the proton–proton collisions at the LHC, b hadrons are produced predominantly in the forward and backward directions with respect to the beam axis, and their kinematic variables are largely uncorrelated. Consequently, the LHCb experiment was designed as a single-arm forward spectrometer covering the rapidity region $2 \leq \eta \leq 5$. The higher cross-section for b-quark production at the LHC compared to that at the B-factories [53,54], translates into larger b-hadron samples available at the LHC. However, the busier environment of the hadron machine means that these measurements contain a much larger amount of background originating from the primary proton-proton interaction vertex. The main strategy to reduce this background is provided by the long lifetime of the b-quark, which, combined with the large boost with which b hadrons are produced, results in a significant displacement between the decay vertices of b hadrons and the primary vertex, At the B-factories, mainly B^0 and B^+ mesons are studied – small samples of B_s^0 mesons are accumulated when running at the $\Upsilon(5S)$ resonance, whose mass sits above the $B_s^0\overline{B_s^0}$ threshold. The hadronization of b-quarks at LHCb gives access to significant samples of other b-hadron species, such as B_s^0 or B_c^+ mesons or Λ_b baryons.

In addition to an incoherent background, a diverse and often abundant array of misreconstructed b-hadron decays that mimic the signal needs to be suppressed with effective selection methods. These selections often rely on the experiments' efficient particle identification capabilities and typically exploit multivariate techniques to combine kinematic and topological features into more powerful variables.

For the study of lepton universality, the ability to identify decays into electrons and muons and to describe the detector response for both final states is required. The latter is a more important challenge for the LHCb experiment, where electron and muon responses differ significantly more than at the B-factories. The trigger is the first important difference between the two experiments. At Belle II, the signature of the $\Upsilon(4S)$ decay means that

the trigger efficiency is close to 100% for events containing b-decays into either muons or electrons [54]. At LHCb, the trigger efficiency varies significantly for the two types of leptons. Muon candidates are triggered by hits left in the muon stations at the far end of the detector, whereas electrons are triggered through their energy deposits in the electromagnetic calorimeter, which suffers from higher occupancy. On average, this results in trigger efficiencies for decays into muons that are around three times larger than those for electrons [55].

The signal extraction in LFU measurements usually relies on some variation of the reconstructed invariant mass of the B candidate, which is used as the final discriminating variable. The resolution in the reconstructed mass is, therefore, another factor central to the precision of LFU measurements, and represents the second important difference between the two experiments. Electron channels are generally reconstructed with worse mass resolution due to the effect of bremsstrahlung radiation, which is more important for electrons than for heavier muons. This effect is emphasised at LHCb due to the larger boost of the b hadron (and, hence, of the decay products) compared to the B-factories. A bremsstrahlung recovery procedure is employed to correct the electron momentum measurement by reconstructing radiated photons around the electron candidate. As shown in Figure 4, the final difference in mass resolution between electrons and muons is small at Belle II. At LHCb, however, the difference between electrons and muons is still significant after the correction, which considerably complicates the LFU analyses.

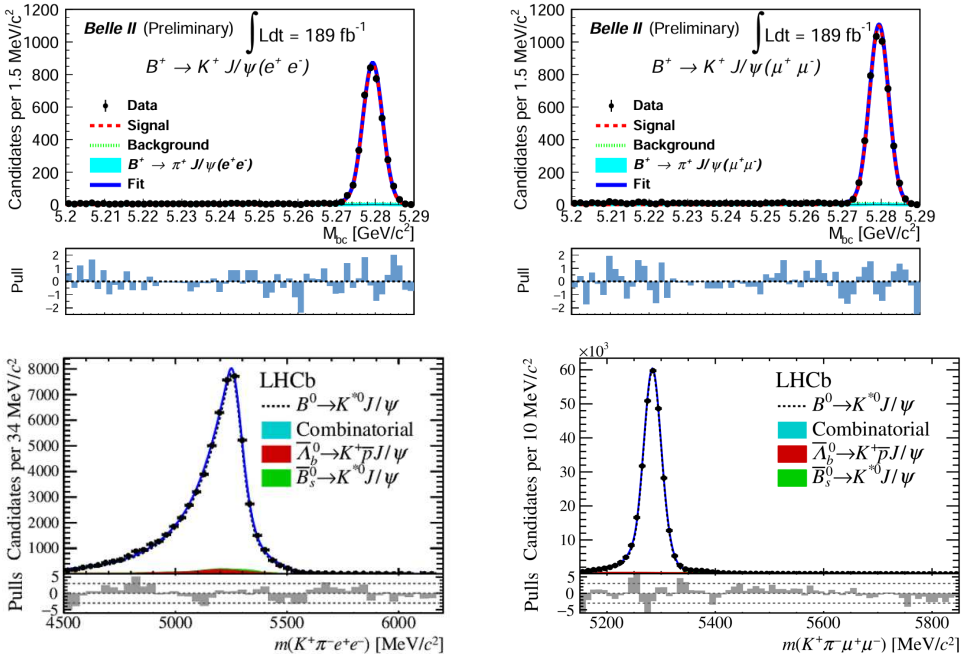

Figure 4. Comparison of the invariant mass resolution for $B \to KJ/\psi(\to ee)$ (**left**) and $B \to KJ/\psi(\to \mu\mu)$ (**right**) decays in Belle II (**top**) and LHCb (**bottom**). While the resolution is similar between electrons and muons in Belle II, it differs significantly in the case of LHCb—note the different x-axis scales in the bottom plots. The pulls below each distribution show the fit residuals normalised to the data uncertainty. Reproduced from [56,57].

Controlling systematic effects, such as uncertainties in the determination of signal efficiencies, presents another challenge. This tends to be more critical in measurements at LHCb, but both experiments use other b-meson decays as control channels to validate the detector response. The accessibility to suitable and high-statistics control modes contributes to the fact that all LFU measurements reported so far are statistically limited. Table 1 summarises the data samples from the different experiments on which these measurements are based.

Table 1. Samples used for LFU measurements in rare b-hadron decay until 2024. The B-factory samples were collected at the $\Upsilon(4S)$ resonance. The LHCb sample is divided into two according to the different centre-of-mass energies of the proton–proton collisions in Run I (7–8 TeV) and Run II (13 TeV) of the LHC.

Experiment	Integrated Luminosity	$b\bar{b}$-Production Cross-Section
BaBar	433 fb^{-1}	1.1 nb
Belle	711 fb^{-1}	1.1 nb
Belle II	190 fb^{-1}	1.1 nb
LHCb Run I	3 fb^{-1}	72 µb
LHCb Run II	6 fb^{-1}	154 µb

3. Semileptonic Decays

The most precise LU tests in rare decays involve the measurement of the ratio of branching ratios of semileptonic $X_b \to h\ell^+\ell^-$ decays, where X_b is a b hadron (B^+, B^0, B_s^0, or Λ_b^0), h represents one or more hadrons, and ℓ is either a muon or an electron. These R_h ratios are defined as follows:

$$R_h = \frac{\int_{q^2\,\mathrm{min}}^{q^2\,\mathrm{max}} \mathcal{B}(X_b \to h\mu^+\mu^-)}{\int_{q^2\,\mathrm{min}}^{q^2\,\mathrm{max}} \mathcal{B}(X_b \to he^+e^-)}\,, \tag{1}$$

and are measured over a range of dilepton invariant mass-squared, $q^2 \in [{q^2}_{\mathrm{min}}, {q^2}_{\mathrm{max}}]$. In the SM, the value of R_h is predicted to be close to unity, owing to the small mass of electrons and muons. Deviations from unity are expected in regions close to the kinematic limits of the decay, specifically at very low q^2 as the dilepton threshold is approached. Estimates of the SM values for the corresponding ratios in $B^+ \to K^+\ell^+\ell^-$ and $B^0 \to K^{*0}\ell^+\ell^-$, R_K and R_{K^*}, are shown in Figure 5. Crucially, the challenges of computing QCD contributions that complicate SM estimates for branching fractions and angular observables do not impact the predictions of the R_h ratios, which benefit from the cancellation of hadronic contributions. The dominant uncertainty is, therefore, driven by QED radiative corrections, which differentially affect the electron and muon modes. These effects are corrected for in the experimental determination using the PHOTOS package [58]. Recent QED calculations [59,60] have estimated the residual uncertainty to be on the order of $\mathcal{O}(1\%)$. Regions where q^2 approaches the mass of the J/ψ and $\psi(2S)$ mesons are excluded from measurements and predictions because they are dominated by tree-level $b \to c\bar{c}s$ resonant processes, such as $B^{+,0} \to K^{+,0}J/\psi$, followed by the $J/\psi \to \ell\ell$ decay.

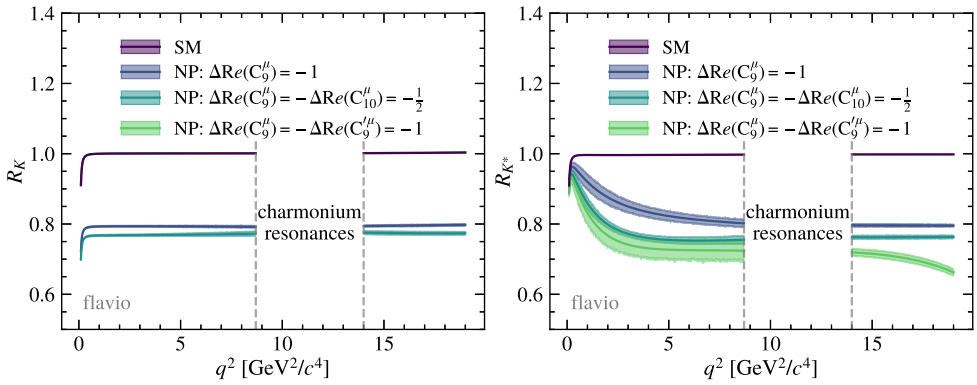

Figure 5. Predictions for R_K (**left**) and R_{K^*} (**right**) in the standard model and different new physics scenarios. Reproduced from [55].

Experimentally, R_h can be determined from the following equation:

$$R_h = \frac{N(X_b \to hee)}{N(X_b \to h\mu\mu)} \frac{\epsilon(X_b \to h\mu\mu)}{\epsilon(X_b \to hee)} \tag{2}$$

where N is the number of decays observed for the corresponding decay and ϵ is the total efficiency with which that decay is reconstructed in the detector. The optimisation of the selection criteria to minimise uncertainty in the signal yields and precise estimation of the signal efficiencies are, therefore, the main drivers of precision.

Measurements at the B-factories suffer from larger statistical uncertainties due to the lower $b\bar{b}$-production cross-section at the e^+e^- machines. On the other hand, measurements in both low and high q^2 have been reported; the latter have so far been measured exclusively in this environment. Current measurements explore $B \to K\ell\ell$ and $B \to K^*\ell\ell$ decays. These include both charged and neutral modes, as the detectors can reconstruct final states with K_S or π^0 mesons with good resolution. The variables commonly used to discriminate the signal from the continuum $B\bar{B}$ background are the beam energy-constrained mass,

$$M_{bc} = \sqrt{E^2_{\text{beam}}/c^4 - |p_B|^2/c^2}, \tag{3}$$

and the energy difference, $\Delta E = E_B - E_{\text{beam}}$, where p_B and E_B are the momentum and energy of the B candidate in the $\Upsilon(4S)$ rest frame and E_{beam} is the beam energy in the centre-of-mass frame. For signal events, the ΔE distribution peaks at zero, whereas the M_{bc} distribution peaks near the B mass. Other variables describing the shape of the event and the topology and kinematics of the signal candidates are also employed to further reduce the continuum background. The combination of requirements in these variables with particle identification information from the detector reduces also the contribution of background from other misreconstructed B decays to negligible levels. Efficiencies are generally extracted using simulation, and the values obtained are validated by calculating the ratio of branching fractions for the corresponding resonant mode [56].

At LHCb, the higher signal yields achieved due to the larger cross-section significantly improve the statistical uncertainty and, hence, the control of the systematic effects becomes the main challenge in the R_h measurements. In particular, the different detector signatures of electrons and muons summarised in Section 2, could lead to sizeable uncertainties in the efficiencies. To reduce these systematic effects, R_h is measured relative to the equivalent ratio for the resonant decay $X_b \to hJ/\psi$,

$$R_h = \frac{\mathcal{B}(X_b \to hee)}{\mathcal{B}(X_b \to h\mu\mu)} \Big/ \frac{\mathcal{B}(X_b \to hJ/\psi(\to \mu\mu))}{\mathcal{B}(X_b \to hJ/\psi(\to ee))} \ , \tag{4}$$

exploiting the fact that $J/\psi \to \ell\ell$ decays have been observed to respect lepton universality within 0.4% [1]. With this approach, R_h can be determined as a double ratio from the observed yields and the relative efficiencies between electrons and muons in the two modes. Furthermore, particle kinematics and detector responses are broadly similar between the rare and resonant modes; hence, the systematic effect of any efficiency mismodelling is expected to largely cancel in the measurement of R_h. The robustness of this approach is illustrated in Figure 6, where the shifts induced by subsequent detector calibrations are compared between the measured ratio of branching ratios for $B^+ \to K^+J/\psi(\to \ell\ell)$ decays, referred to as *single ratio* or $r^K_{J/\psi}$, and the measured double ratio, R_K [55]. While systematic variations can induce shifts of $\mathcal{O}(20\%)$ in the single ratio, the double ratio remains insensitive. Additional resonant modes are used for calibration and cross-checking in different q^2 regions. The $X_b \to H\psi(2S)(\to \ell\ell)$ decays can be employed at high q^2 values, while the charm decays $D^+_{(s)} \to \pi^+\phi(\to \ell\ell)$ have recently been used as a validation of the approach at low q^2 [61].

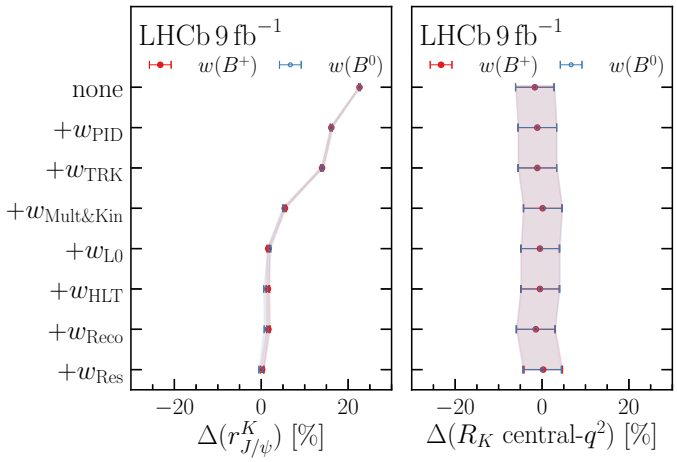

Figure 6. Effect of the different steps of the efficiency calibration on the measured single ratio for the resonant mode (**left**), $r^K_{J/\psi}$, and the double ratio (**right**), R_K, as defined in (4). Reproduced from [55].

The invariant mass of the reconstructed X_b candidates is used to extract the yield of the different processes. Here, the relevance of the bremsstrahlung losses for electrons in LHCb constitutes the second challenge of the analysis. Even with the bremsstrahlung recovery procedure introduced in Section 2, the invariant mass of the electron signals is still degraded, as illustrated in Figure 7. This degradation complicates the separation between the signal and background contributions, which may come from random combinations of reconstructed particles or misreconstructed B-decays. In particular, substantial leakage from the J/ψ charmonium resonant mode is observed, even after the imposed q^2 veto. At high-q^2, leakage from the $\psi(2S)$ resonance makes measurements more challenging.

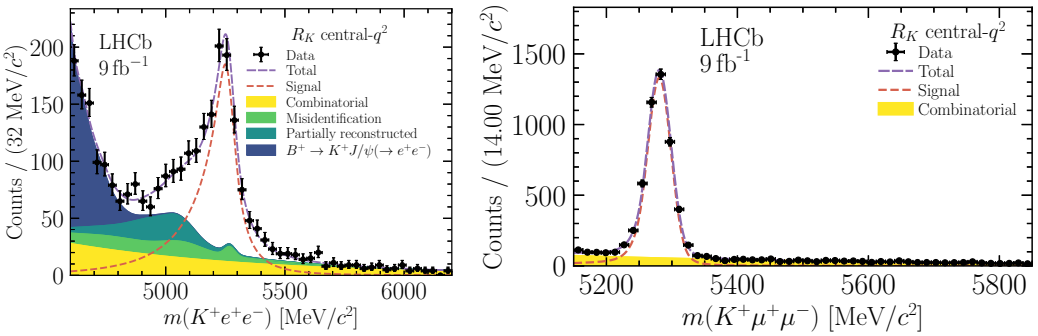

Figure 7. Invariant mass distribution for $B^+ \to K^+e^+e^-$ (**left**) and $B^+ \to K^+\mu^+\mu^-$ (**right**) candidates with $q^2 \in [1.1, 6.0]$ GeV$^2/c^4$ at LHCb. Reproduced from [55].

Background contributions from other b-hadron decays arising from particle misidentification could accumulate at the true X_b mass and, hence, bias the determination of the signal yield. Misidentification of hadrons as electrons is especially dangerous when studying electron channels. Electron identification, provided mainly by the electromagnetic calorimeter in LHCb, can achieve efficiencies of 80 to 90%, and small misidentification rates at the sub-percent level [62]. However, contributions from fully hadronic B decays, where two of the hadrons are misidentified as electrons, can still be significant, since the branching fractions for these decays can be up to three orders of magnitude higher than that of the signal electron mode. In the most recent R_K and R_{K^*} measurement [55], the stability of the result with respect to the electron identification criteria was crucial for identifying an issue with the underestimation of these backgrounds, and the consequent overestimation of the electron mode yield, in previous analyses [63]. A data-driven method was used to constrain the contribution from particle misidentification backgrounds in the final signal fit, as seen in Figure 7.

Measurements of R_K and R_{K^*} have been performed by LHCb [55,64,65] in the low-q^2 region and BaBar [66], Belle [67–69], and Belle II [70] in both low- and high-q^2 regions. In addition, LHCb has measured the corresponding ratios in $\Lambda_b^0 \to pK^-\ell^+\ell^-$ [71]. All of these results, summarised in Figure 8, remain statistically limited. Recently, the R_K ratio has also been measured by the CMS experiment [72] using a dedicated trigger strategy to collect samples enriched in b-hadron decays. Even though this measurement is still not competitive with those from other experiments, it showcases an interesting possibility for future b-physics studies at the LHC. A scan of the results in Figure 8 shows good agreement with lepton universality, with most measurements agreeing with the SM prediction within 1–2σ.

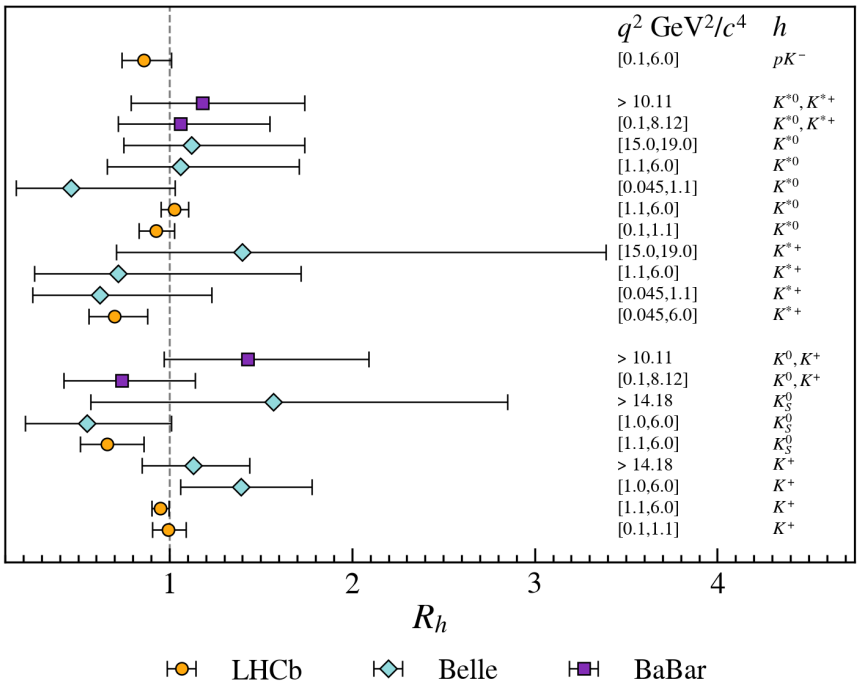

Figure 8. Summary of LU tests in the ratio of branching ratios of $b \to s\mu^+\mu^-$ and $b \to se^+e^-$ transitions. Measurements from BaBar [66], Belle [67–69], and LHCb [55,64,65,71] are shown.

Angular Observables

Aside from the branching ratios, rare semileptonic decays offer a number of additional observables that can be determined from the study of the angular distribution of the decay products. See, for example, Ref. [73] for a complete account of the accessible observables in $B \to K^+\pi^-\ell\ell$. These observables have different sensitivities to NP contributions and can also be used to test models including lepton universality violation [74].

In particular, the decay $B^0 \to K^{*0}\mu^+\mu^-$ has been extensively studied in recent years [10–15]. This decay can be fully described as a function of the invariant mass squared of the muon pair, q^2, and three decay angles θ_K, θ_ℓ, and ϕ (see [75] for a full description of these variables). On this basis, the differential decay rate can be expressed in terms of eight observables: F_L, the longitudinal polarisation fraction of the K^{*0}, A_{FB}, the forward–backward asymmetry of the dilepton system, and the S_i observables with $i = 3, 4, 5, 7, 8, 9$ [12]. From these, an additional set of optimised observables, P_i, can be defined, in which the leading-order form factor uncertainties cancel [76].

In the most recent LHCb analysis of the $B^0 \to K^{*0}\mu^+\mu^-$ decay [9], a full comparison of the angular observables with the corresponding SM predictions indicates that the data would favour a modified $b \to s$ vector coupling strength. Interestingly, this modification would also help alleviate other tensions observed in measurements of branching ratios and angular distributions in other $b \to s\ell^+\ell^-$ transitions [5–8,18,19]. To test whether this

potential NP contribution is lepton-universal, a comparison of these measurements with the equivalent ones for $B^0 \to K^{*0} e^+ e^-$ is required.

The Belle experiment studied the angular distribution of $B^{0,+} \to K^{*0,+} \ell^+ \ell^-$ decays using the full $\Upsilon(4S)$ data sample, combining the $K^{*0} \to K^+ \pi^-$, $K^{*+} \to K^+ \pi^0$, and $K^{*+} \to K^0_S \pi^+$ final states [16]. Due to limited statistics in the sample, with 127 ± 15 and 185 ± 17 signal candidates obtained for the electron and muon channels, respectively, a folding technique was employed to extract a subset of the angular observables [77,78]. This transformation is applied to certain regions of the angular space, exploiting the symmetries of the system to simplify the expression for the differential decay rate. The analysis measured the optimised observables, P'_4 and P'_5, in four q^2 bins, for both the electron and muon modes, as well as the difference between lepton flavours, Q_4 and Q_5 [74]. Figure 9 shows the comparison between electrons and muons for the P'_5 observable, and the measurement of Q_5, which, as expected, is predicted with more precision in the SM. The results were found to be compatible with the SM predictions within the statistical precision, with the largest tension observed in the muon P'_5 observable at the 2.6σ level. Further measurements of these and other Q_i observables from Belle II and LHCb are, therefore, highly anticipated.

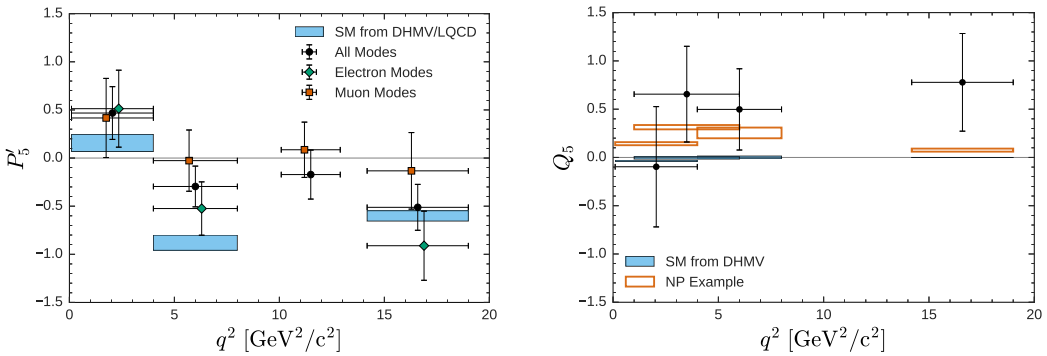

Figure 9. Measurements of the P'_5 observable in $B^0 \to K^{*0} e^+ e^-$ and $B^0 \to K^{*0} \mu^+ \mu^-$ decays and their combination (**left**) and the LU observable $Q_5 = P'_5(\mu) - P'_5(e)$ (**right**). The results from the Belle experiment are compared with the SM predictions [74,79]. Reproduced from [16].

4. Fully Leptonic Decays

The leptonic $B_{(s)} \to \ell\ell$ decays are even rarer in the SM than their semileptonic counterparts due to helicity suppression. This suppression, which scales with m_ℓ / m_b, affects decays into μ, e, and τ leptons differently. As these processes contain only leptons in the final state, predictions of the branching fractions can be made very accurately within the SM [80,81]:

$$\mathcal{B}(B^0_s \to ee) = (8.54 \pm 0.55) \times 10^{-14} \qquad \mathcal{B}(B^0 \to ee) = (2.48 \pm 0.21) \times 10^{-15} \quad (5)$$

$$\mathcal{B}(B^0_s \to \mu\mu) = (3.66 \pm 0.14) \times 10^{-9} \qquad \mathcal{B}(B^0 \to \mu\mu) = (1.03 \pm 0.05) \times 10^{-9} \quad (6)$$

$$\mathcal{B}(B^0_s \to \tau\tau) = (7.73 \pm 0.49) \times 10^{-7} \qquad \mathcal{B}(B^0 \to \tau\tau) = (2.22 \pm 0.19) \times 10^{-9}. \quad (7)$$

For this reason, these decays are powerful probes for NP contributions mediated, for example, by leptoquarks, heavy Z' bosons, or exotic Higgs bosons [82]. In particular, new scalar contributions breaking the helicity suppression would contribute to lepton non-universality in these decays.

Experimentally, $B_s^0 \to \mu\mu$ is the only one of these decays that has been observed so far. The most precise determination of its branching fraction has come from the LHC, with measurements from ATLAS [83], CMS [84], and LHCb [85] yielding the following:

$$\mathcal{B}(B_s^0 \to \mu\mu)^{\text{ATLAS}} = (2.8^{+0.8}_{-0.7}(\text{stat} + \text{syst})) \times 10^{-9} \quad (8)$$

$$\mathcal{B}(B_s^0 \to \mu\mu)^{\text{CMS}} = (3.83^{+0.38}_{-0.36}\,(\text{stat})^{+0.19}_{-0.16}(\text{syst})\,^{+0.14}_{-0.13}(f_s/f_u)) \times 10^{-9} \quad (9)$$

$$\mathcal{B}(B_s^0 \to \mu\mu)^{\text{LHCb}} = (3.09^{+0.46}_{-0.43}(\text{stat})\,^{+0.15}_{-0.11}(\text{syst})) \times 10^{-9}, \quad (10)$$

where the uncertainties are statistical (stat), systematic (syst), and related to the ratio of hadronisation fractions (f_s/f_u), which is needed when decays from different B-meson species are used as normalisation. All of these measurements are in good agreement with the SM predictions. As part of these analyses, searches for the further suppressed $B^0 \to \mu\mu$ decay are performed. No evidence has been found for this decay yet, and the best limit on its branching ratio is estimated at $\mathcal{B}(B^0 \to \mu + \mu-) < 1.2 \times 10^{-10}$ at a 95% confidence level (CL) [85]. For a detailed discussion of these measurements, see the dedicated article in this issue [86].

Searches for $B^0_{(s)} \to e^+e^-$ decays have been performed at the LHCb experiment using data collected during Run I and Run II of the LHC, corresponding to a total of $5\,\text{fb}^{-1}$. The strategy of these searches closely follows that of other measurements with electrons at LHCb, where the search is divided into several categories based on the data-taking conditions and whether the energy of the electron has been corrected using reconstructed bremsstrahlung photons. Apart from combinatorial background, the main source of background in the signal region arises from the misidentification of hadrons from $B \to \pi e\nu$ and $B \to hh'$ decays, where h represents pions or kaons. These predominantly contribute to the categories where bremsstrahlung photons have been added to (at most) one electron, and are included in the fit to the B-meson reconstructed invariant mass used to extract the observed signal yield. In order to reduce systematic uncertainties, this yield is then normalised to that of the decay $B^+ \to K^+ J\psi$ with the $J/\psi \to e^+e^-$. No significant signal is found for either the B^0 or B_s^0 meson, and the following limits on the branching fractions are calculated as follows: $\mathcal{B}(B_s^0 \to e^+e^-) < 9.4(11.2) \times 10^{-9}$ and $B(B^0 \to e^+e^-) < 2.5(3.0) \times 10^{-9}$ at 90 (95) % CL. Each limit assumes no contribution from the other corresponding decay. These limits are far from the SM prediction but begin to probe regions of interest for many NP models.

5. Decays Involving τ Leptons

The previous sections focused on comparisons between the properties of decays involving electrons and muons. Of course, comparisons between taus and the lighter leptons are equally powerful probes for NP. Furthermore, tension with the LU prediction in tree-level decays of type $b \to c\ell^-\overline{\nu}_\ell$ has been demonstrated in several experiments. In particular, the observables $R(D)$ and $R(D^*)$, defined as the ratio of branching fractions of $B \to D^{(*)}\tau^+\nu_\tau$ and $B \to D^{(*)}\mu^+\nu_\mu$ decays, are predicted to be 0.298 ± 0.004 and 0.254 ± 0.005 in the SM [87], and differ from unity mainly because of phase-space effects due to the $\tau - \mu$ mass difference. Measurements of these quantities performed by the BaBar, Belle, and LHCb collaborations [36–45] showed an excess with respect to the SM prediction, as can be seen in Figure 10. It has been highlighted that under fairly model-independent assumptions, NP contributions attempting to resolve the tension in $b \to c\ell^-\overline{\nu}_\ell$ transitions would also significantly enhance $b \to s\tau^+\tau^-$ processes [46]. Furthermore, higher-order contributions of the same type of NP could also induce lepton-universal effects in $b \to s\mu^+\mu^-$ and $b \to se^+e^-$ transitions, which could help address the anomalies observed while respecting the bounds from LU ratios presented in the previous sections [47].

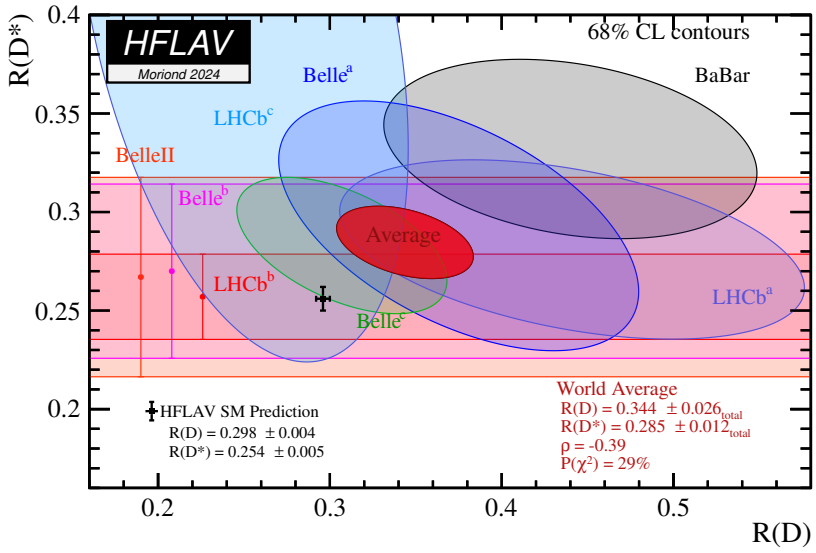

Figure 10. $R(D)$ and $R(D^*)$ measurements and averages compared to the SM prediction [87].

Experimentally, τ leptons are reconstructed through their leptonic or hadronic decays, as their lifetime is too short to be directly detected. Due to the multiple neutrinos in the final state, the invariant mass signature for these decays does not exhibit a peaking structure, making these searches significantly more challenging than those involving electrons or muons. This explains why, although their branching ratio is predicted to be on the order of $\mathcal{O}(10^{-7})$ in the SM, no such process has been observed so far.

Searches for semileptonic $B \to K^+\tau^+\tau^-$ decays have been performed at B-factories [88] using only leptonic decays of the tau: $\tau^- \to \mu^-\bar{\nu}_\mu\nu_\tau$ and $\tau^- \to e^-\bar{\nu}_e\nu_\tau$. In this analysis, the accompanying B-meson is reconstructed exclusively via its decay into one of several hadronic decay modes. This provides a measurement of the missing energy carried away by the neutrinos, which allows discrimination against multiple backgrounds. In addition, a dedicated neural network selection targets background events containing semileptonic $b \to c\ell^-\bar{\nu}_\ell$ decays, such as $B \to D^{(*)}\ell\bar{\nu}_\ell$ with $D^{(*)} \to K\ell'\bar{\nu}_{\ell'}$, which have the same detected final-state particles as signal events as well as missing energy. No significant signal was observed and the upper limit $\mathcal{B}(B^+ \to K^+\tau^+\tau^-) < 2.25 \times 10^{-3}$ at 90% CL was set.

LHCb has performed a search for the fully leptonic decays $B_s^0 \to \tau\tau$ and $B^0 \to \tau\tau$, where the τ is reconstructed through its hadronic decay into three charged pions and a neutrino, assuming specific intermediate resonances: $\tau^- \to a_1^-(\rho^0\pi^-)\nu_\tau$. For this analysis, a multivariate classifier combines kinematic and topological information of the decay and allows the signal yield to be extracted. In particular, the amplitude structure of the tau hadronic decay is exploited to define control regions that allow better control of the background in the signal-enriched regions. No signal was observed here either, and the 95% CL upper limits $B(B_s^0 \to \tau\tau) < 3.0 \times 10^{-3}$ and $B(B^0 \to \tau\tau) < 1.3 \times 10^{-3}$ were set [89].

In both cases, the branching ratio limits are far from the predictions based on lepton universality. The large datasets expected from Belle II and the upgrades at LHCb, combined with significant efforts to improve tau reconstruction techniques, will help enhance these limits. These improvements will begin to probe interesting areas of parameter space in many NP models, though they will most likely remain above the SM predictions.

6. Prospects

In the coming years, larger samples of $b \to s\ell^+\ell^-$ decays will become available, which will allow significant improvements in the precision of LU observables, as well as the exploration of new measurements currently hindered by the lack of statistical power.

The Belle II experiment is expected to collect a data sample of 50 ab^{-1} [90] by 2035, which will significantly improve the precision of the LU ratios. The statistical sensitivity

values in R_K and R_{K^*} are expected to be below 2% for the entire q^2 region and approximately 3% for $q^2 \in [1-6]\,\mathrm{GeV}^2/c^4$, with the full data sample [91].

The LHCb experiment has resumed data taking after a detector upgrade, enabling operation at a data rate approximately five times higher than in Run II [92]. It is expected that a sample corresponding to $50\,\mathrm{fb}^{-1}$ will be collected by the end of Run IV. With this data sample, the expected statistical precision in R_K and R_{K^*} is expected to reach the percent level [93]. Thus, a second upgrade is planned to fully exploit the capabilities of the high-luminosity LHC, where the data rate will increase by an additional order of magnitude, collecting a total sample corresponding to $300\,\mathrm{fb}^{-1}$. The measurements of angular observables in $b \to se^+e^-$ decays will significantly benefit from this, where a precision comparable to that of the corresponding $b \to s\mu^+\mu^-$ modes today will become accessible [93].

The additional data will also enable extending the study of lepton universality to the further suppressed $b \to d\ell^+\ell^-$ transitions. While processes with final-state muons have been observed by LHCb [94–96], no evidence for equivalent modes with electrons has been found to date [1,97]. The first observation of $B^+ \to \pi^+e^+e^-$ could soon be within reach for both Belle II and LHCb, if LU is respected. A precise measurement of $R_\pi = \mathcal{B}(B^+ \to \pi^+\mu^+\mu^-)/\mathcal{B}(B^+ \to \pi^+e^+e^-)$ will likely need to wait until the end of LHCb's second upgrade, where statistical precision of a few percent could be achieved [93].

In the future, the proposed Future Circular Collider (FCC) at CERN could significantly impact LU studies in rare b-decays. The proposal includes an initial phase, running in electron–positron mode (FCC-ee), with the machine operating at centre-of-mass energies ranging from the Z-pole (91 GeV) and the $t\bar{t}$ threshold (365 GeV). Such a machine would offer the opportunity to accumulate unprecedented samples of b-quarks when operating at the Z-pole, owing to the large production rate of Z-bosons and the large branching ratio of the $Z \to b\bar{b}$ decay. In addition, the initial energy constraint from the resonant production would provide ideal conditions for measurements of decays with missing energy, such as those involving $b \to s\tau\tau$ transitions [98] or $b \to s\nu\bar{\nu}$ processes [99].

7. Conclusions

The observation of lepton-flavour non-universality would be a clear indicator of physics beyond the standard model. Tests of lepton universality in rare b-hadron decays, mediated by FCNC $b \to s(d)\ell^+\ell^-$ transitions, are particularly sensitive to new physics scenarios at high energy scales. Despite earlier hints of tensions with the standard model predictions, no indication of lepton-universality violation in these decays has been found so far. Further improvements in these measurements and the exploration of additional $b \to s(d)\ell^+\ell^-$ processes and observables remain well-motivated. Future datasets from the Belle II and LHCb experiments hold great potential for precise exploration of lepton universality in these transitions.

Author Contributions: Writing, review, and editing by P.Á.C. and R.M.W. All authors have read and agreed to the published version of the manuscript.

Funding: P.A.C. and R.M.W. are supported by STFC, UK.

Data Availability Statement: No new data were created or analysed in this work.

Acknowledgments: The authors thank Samuel Cunliffe for the discussions about the Belle II experiment. We also thank the Belle, Belle II, and LHCb collaborations for permitting the reproduction of their results in this review.

Conflicts of Interest: The authors declare no conflicts of interest.

References

1. Particle Data Group. Review of particle physics. *PTEP* **2022**, *2022*, 083C01. [CrossRef]
2. Jung, M.; Pich, A.; Tuzon, P. Charged-Higgs phenomenology in the aligned two-Higgs-doublet model. *J. High Energy Phys.* **2010**, *11*, 003. [CrossRef]

3. Hiller, G.; Schmaltz, M. R_K and future $b \to s\ell\ell$ physics beyond the standard model opportunities. *Phys. Rev. D* **2014**, *90*, 054014. [CrossRef]
4. Tanaka, M. Charged Higgs effects on exclusive semi-tauonic B decays. *Zeitschrift für Physik C Particles and Fields* **1995**, *67*, 321–326. [CrossRef]
5. LHCb Collaboration. Branching fraction measurements of the rare $B_s^0 \to \phi\mu^+\mu^-$ and $B_s^0 \to f_2'(1525)\mu^+\mu^-$ - decays. *Phys. Rev. Lett.* **2021**, *127*, 151801. [CrossRef]
6. LHCb Collaboration. Measurements of the S-wave fraction in $B^0 \to K^+\pi^-\mu^+\mu^-$ decays and the $B^0 \to K^*(892)^0\mu^+\mu^-$ differential branching fraction. *JHEP* **2016**, *11*, 047; Erratum in: *JHEP* **2017**, *04*, 142. [CrossRef]
7. LHCb Collaboration. Differential branching fraction and angular analysis of $\Lambda_b^0 \to \Lambda\mu^+\mu^-$ decays. *JHEP* **2015**, *06*, 115; Erratum in: JHEP **2018**, *09*, 145. [CrossRef]
8. LHCb Collaboration. Differential branching fractions and isospin asymmetries of $B \to K^{(*)}\mu^+\mu^-$ decays. *JHEP* **2014**, *06*, 133. [CrossRef]
9. LHCb Collaboration. Measurement of *CP*-averaged observables in the $B^0 \to K^{*0}\mu^+\mu^-$ decay. *Phys. Rev. Lett.* **2020**, *125*, 011802. [CrossRef]
10. CMS Collaboration. Measurement of angular parameters from the decay $B^0 \to K^{*0}\mu^+\mu^-$ in proton-proton collisions at $\sqrt{s} = 8$ TeV. *Phys. Lett. B* **2018**, *781*, 517–541. [CrossRef]
11. ATLAS Collaboration. Angular analysis of $B_d^0 \to K^*\mu^+\mu^-$ decays in pp collisions at $\sqrt{s} = 8$ TeV with the ATLAS detector. *JHEP* **2018**, *10*, 047, [CrossRef]
12. LHCb Collaboration. Angular analysis of the $B^0 \to K^{*0}\mu^+\mu^-$ decay using 3 fb^{-1} of integrated luminosity. *JHEP* **2016**, *02*, 104, [CrossRef]
13. BaBar Collaboration. Measurements of branching fractions, rate asymmetries, and angular distributions in the rare decays $B \to K\ell^+\ell^-$ and $B \to K^*\ell^+\ell^-$. *Phys. Rev. D* **2006**, *73*, 092001. [CrossRef]
14. Belle Collaboration. Measurement of the differential branching fraction and forward-backward asymmetry for $B \to K^{(*)}\ell^+\ell^-$. *Phys. Rev. Lett.* **2009**, *103*, 171801. [CrossRef]
15. CDF Collaboration. Measurements of the angular distributions in the decays $B \to K^{(*)}\mu^+\mu^-$ at CDF. *Phys. Rev. Lett.* **2012**, *108*, 081807. [CrossRef]
16. Belle Collaboration. Lepton-flavor-dependent angular analysis of $B \to K^*\ell^+\ell^-$. *Phys. Rev. Lett.* **2017**, *118*, 111801. [CrossRef]
17. LHCb Collaboration. Angular moments of the decay $\Lambda_b^0 \to \Lambda\mu^+\mu^-$ at low hadronic recoil. *JHEP* **2018**, *09*, 146. [CrossRef]
18. LHCb Collaboration. Angular analysis of the $B^+ \to K^{*+}\mu^+\mu^-$ decay. *Phys. Rev. Lett.* **2021**, *126*, 161802. [CrossRef]
19. LHCb Collaboration. Angular analysis of the rare decay $B_s^0 \to \phi\mu^+\mu^-$. *JHEP* **2021**, *11*, 043. [CrossRef]
20. Gubernari, N.; Reboud, M.; van Dyk, D.; Virto, J. Improved theory predictions and global analysis of exclusive $b \to s\mu^+\mu^-$ processes. *JHEP* **2022**, *09*, 133. [CrossRef]
21. Greljo, A.; Salko, J.; Smolkovič, A.; Stangl, P. Rare b decays meet high-mass Drell-Yan. *JHEP* **2023**, *05*, 087. [CrossRef]
22. Algueró, M.; Biswas, A.; Capdevila, B.; Descotes-Genon, S.; Matias, J.; Novoa-Brunet, M. To (b)e or not to (b)e: no electrons at LHCb. *Eur. Phys. J. C* **2023**, *83*, 648. [CrossRef]
23. Ciuchini, M.; Fedele, M.; Franco, E.; Paul, A.; Silvestrini, L.; Valli, M. Constraints on lepton universality violation from rare B decays. *Phys. Rev. D* **2023**, *107*, 055036. [CrossRef]
24. Jäger, S.; Martin Camalich, J. Reassessing the discovery potential of the $B \to K^*\ell^+\ell^-$ decays in the large-recoil region: SM challenges and BSM opportunities. *Phys. Rev. D* **2016**, *93*, 014028. [CrossRef]
25. Lyon, J.; Zwicky, R. Resonances gone topsy turvy-the charm of QCD or new physics in $b \to s\ell^+\ell^-$? *arXiv* **2014**. [arXiv:hep-ph/1406.0566].
26. Ciuchini, M.; Fedele, M.; Franco, E.; Mishima, S.; Paul, A.; Silvestrini, L.; Valli, M. $B \to K^*\ell^+\ell^-$ decays at large recoil in the Standard Model: A theoretical reappraisal. *JHEP* **2016**, *06*, 116. [CrossRef]
27. Bobeth, C.; Chrzaszcz, M.; van Dyk, D.; Virto, J. Long-distance effects in $B \to K^*\ell\ell$ from analyticity. *Eur. Phys. J. C* **2018**, *78*, 451. [CrossRef]
28. CMS Collaboration. Precision measurement of the W boson decay branching fractions in proton-proton collisions at $\sqrt{s} = 13$ TeV. *Phys. Rev. D* **2022**, *105*, 072008. [CrossRef]
29. ATLAS Collaboration. Test of the universality of τ and μ lepton couplings in W-boson decays with the ATLAS detector. *Nature Phys.* **2021**, *17*, 813–818. [CrossRef]
30. Pich, A. Precision tau physics. *Prog. Part. Nucl. Phys.* **2014**, *75*, 41–85. [CrossRef]
31. ATLAS Collaboration. Precision measurement and interpretation of inclusive W^+ , W^- and Z/γ^* production cross sections with the ATLAS detector. *Eur. Phys. J. C* **2017**, *77*, 367. [CrossRef]
32. CDF Collaboration. Measurements of inclusive W and Z cross sections in p anti-p collisions at s**(1/2) = 1.96-TeV. *J. Phys. G* **2007**, *34*, 2457–2544. [CrossRef]
33. ALEPH, DELPHI, L3, OPAL, SLD, LEP Electroweak Collaborations, SLD Electroweak Group, SLD Heavy Flavour Group. Precision electroweak measurements on the Z resonance. *Phys. Rept.* **2006**, *427*, 257–454. [CrossRef]
34. ALEPH, DELPHI, L3, OPAL, LEP Electroweak Collaborations. Electroweak Measurements in Electron-Positron Collisions at W-Boson-Pair Energies at LEP. *Phys. Rept.* **2013**, *532*, 119–244. [CrossRef]
35. LHCb Collaboration. Measurement of forward $W \to e\nu$ production in pp collisions at $\sqrt{s} = 8$ TeV. *JHEP* **2016**, *10*, 030. [CrossRef]

36. BaBar Collaboration. Evidence for an Excess of $\overline{B} \to D^{(*)}\tau^-\overline{\nu}_\tau$ Decays. *Phys. Rev. Lett.* **2012**, *109*, 101802. [CrossRef] [PubMed]
37. BaBar Collaboration. Measurement of an excess of $\overline{B} \to D^{(*)}\tau^-\overline{\nu}_\tau$ decays and implications for charged Higgs bosons. *Phys. Rev. D* **2013**, *88*, 072012. [CrossRef]
38. Belle Collaboration. Measurement of the branching ratio of $\overline{B} \to D^{(*)}\tau^-\overline{\nu}_\tau$ relative to $\overline{B} \to D^{(*)}\ell^-\overline{\nu}_\ell$ decays with hadronic tagging at Belle. *Phys. Rev. D* **2015**, *92*, 072014. [CrossRef]
39. Belle Collaboration. Measurement of the τ Lepton Polarization and $R(D^*)$ in the Decay $\overline{B} \to D^*\tau^-\overline{\nu}_\tau$. *Phys. Rev. Lett.* **2017**, *118*, 211801. [CrossRef]
40. Belle Collaboration. Measurement of the τ lepton polarization and $R(D^*)$ in the decay $\overline{B} \to D^*\tau^-\overline{\nu}_\tau$ with one-prong hadronic τ decays at Belle. *Phys. Rev. D* **2018**, *97*, 012004. [CrossRef]
41. Belle Collaboration. Measurement of $\mathcal{R}(D)$ and $\mathcal{R}(D^*)$ with a semileptonic tagging method. *Phys. Rev. Lett.* **2020**, *124*, 161803. [CrossRef] [PubMed]
42. Belle II Collaboration. A test of lepton flavor universality with a measurement of $R(D^*)$ using hadronic B tagging at the Belle II experiment. *arXiv* **2024**. [arXiv:hep-ex/2401.02840].
43. LHCb Collaboration. Measurement of the ratios of branching fractions $\mathcal{R}(D^*)$ and $\mathcal{R}(D^0)$. *Phys. Rev. Lett.* **2023**, *131*, 111802. [CrossRef]
44. LHCb Collaboration. Test of lepton flavor universality using $B^0 \to D^{*-}\tau^+\nu_\tau$ decays with hadronic τ channels. *Phys. Rev. D* **2023**, *108*, 012018. [CrossRef]
45. LHCb Collaboration. Measurement of the branching fraction ratios $R(D^+)$ and $R(D^{*+})$ using muonic τ decays. *arXiv* **2024**. [arXiv:hep-ex/2406.03387].
46. Capdevila, B.; Crivellin, A.; Descotes-Genon, S.; Hofer, L.; Matias, J. Searching for new physics with $b \to s\tau^+\tau^-$ processes. *Phys. Rev. Lett.* **2018**, *120*, 181802. [CrossRef]
47. Crivellin, A.; Greub, C.; Müller, D.; Saturnino, F. Importance of loop effects in explaining the accumulated evidence for new physics in B decays with a vector leptoquark. *Phys. Rev. Lett.* **2019**, *122*, 011805. [CrossRef] [PubMed]
48. Aebischer, J.; Isidori, G.; Pesut, M.; Stefanek, B.A.; Wilsch, F. Confronting the vector leptoquark hypothesis with new low- and high-energy data. *Eur. Phys. J. C* **2023**, *83*, 153. [CrossRef] [PubMed]
49. Waheed, E. Belle II experiment: status and prospects. *PoS* **2022**, *405*, 031. [CrossRef]
50. LHCb Collaboration. The LHCb Detector at the LHC. *J. Instrum.* **2008**, *3*, S08005. [CrossRef]
51. ATLAS Collaboration. The ATLAS experiment at the CERN Large Hadron Collider. *J. Instrum.* **2008**, *3*, S08003. [CrossRef]
52. CMS Collaboration. The CMS experiment at the CERN LHC. *J. Instrum.* **2008**, *3*, S08004. [CrossRef]
53. LHCb Collaboration. Measurement of the b-quark production cross-section in 7 and 13 TeV pp collisions. *Phys. Rev. Lett.* **2017**, *118*, 052002, Erratum in: *Phys. Rev. Lett.* **2017**, *119*, 169901. [CrossRef]
54. Belle II Collaboration. The Belle II Physics Book. *PTEP* **2019**, *2019*, 123C01; Erratum in: PTEP **2020**, *2020*, 029201. [CrossRef]
55. LHCb Collaboration. Measurement of lepton universality parameters in $B^+ \to K^+\ell^+\ell^-$ and $B^0 \to K^{*0}\ell^+\ell^-$ decays. *Phys. Rev. D* **2023**, *108*, 032002. [CrossRef]
56. Belle II Collaboration. Measurements of the branching fraction, isospin asymmetry, and lepton-universality ratio in $B \to J/\psi K$ decays at Belle II. *arXiv* **2022**. [arXiv:hep-ex/2207.11275].
57. LHCb Collaboration. Test of lepton universality with $B^0 \to K^{*0}\ell^+\ell^-$ decays. *JHEP* **2017**, *08*, 055. [CrossRef]
58. Golonka, P.; Was, Z. PHOTOS Monte Carlo: A Precision tool for QED corrections in Z and W decays. *Eur. Phys. J. C* **2006**, *45*, 97–107. [CrossRef]
59. Bordone, M.; Isidori, G.; Pattori, A. On the Standard Model predictions for R_K and R_{K^*}. *Eur. Phys. J. C* **2016**, *76*, 440. [CrossRef]
60. Isidori, G.; Nabeebaccus, S.; Zwicky, R. QED corrections in $\overline{B} \to \overline{K}\ell^+\ell^-$ at the double-differential level. *JHEP* **2020**, *12*, 104. [CrossRef]
61. LHCb Collaboration. Measurements of the branching fraction ratio $\mathcal{B}(\prec \to \preceq^+\preceq^-)/\mathcal{B}(\prec \to \rceil^+\rceil^-)$ with charm meson decays. *arXiv* **2024**. [arXiv:hep-ex/2402.01336].
62. Abellán Beteta, C.; Alfonso Albero, A.; Amhis, Y.; Barsuk, S.; Beigbeder-Beau, C.; Belyaev, I.; Bonnefoy, R.; Breton, D.; Callot, O.; Calvo Gomez, M.; et al. Calibration and performance of the LHCb calorimeters in Run 1 and 2 at the LHC. *arXiv* **2020**. [arXiv:physics.ins-det/2008.11556].
63. LHCb Collaboration. Test of lepton universality in beauty-quark decays. *Nature Phys.* **2022**, *18*, 277–282; Addendum: *Nature Phys.* **2023**, *19*. [CrossRef]
64. LHCb Collaboration. Test of lepton universality in $b \to s\ell^+\ell^-$ decays. *Phys. Rev. Lett.* **2023**, *131*, 051803. [CrossRef]
65. LHCb Collaboration. Tests of lepton universality using $B^0 \to K^0_S\ell^+\ell^-$ and $B^+ \to K^{*+}\ell^+\ell^-$ decays. *Phys. Rev. Lett.* **2022**, *128*, 191802. [CrossRef]
66. BaBar Collaboration. Measurement of Branching Fractions and Rate Asymmetries in the Rare Decays $B \to K^{(*)}l^+l^-$. *Phys. Rev. D* **2012**, *86*, 032012. [CrossRef]
67. Belle Collaboration. Measurement of the differential branching fraction and forward-backward asymmetry for $B \to K^{(*)}\ell^+\ell^-$. *arXiv* **2008**. [arXiv:hep-ex/0810.0335].
68. Belle II Collaboration. Test of lepton flavor universality and search for lepton flavor violation in $B \to K\ell\ell$ decays. *J. High Energy Phys.* **2021**, *2021*, 105. [CrossRef]

69. Belle Collaboration. Test of lepton-flavor universality in $B \to K^* \ell^+ \ell^-$ Decays at Belle. *Phys. Rev. Lett.* **2021**, *126*, 161801. [CrossRef] [PubMed]
70. Belle II Collaboration. Measurement of the branching fraction for the decay $B \to K^*(892)\ell^+\ell^-$ at Belle II. *arXiv* **2022**. [arXiv:hep-ex/2206.05946].
71. LHCb Collaboration. Test of lepton universality with $\Lambda_b^0 \to pK^-\ell^+\ell^-$ decays. *JHEP* **2020**, *05*, 040. [CrossRef]
72. CMS Collaboration. Test of lepton flavor universality in $B^{\pm} \to K^{\pm}\mu^+\mu^-$ and $B^{\pm} \to K^{\pm}e^+e^-$ decays in proton-proton collisions at $\sqrt{s}$ = 13 TeV. *arXiv* **2024**. [arXiv:hep-ex/2401.07090].
73. Algueró, M.; Alvarez Cartelle, P.; Marshall, A.M.; Masjuan, P.; Matias, J.; McCann, M.A.; Patel, M.; Petridis, K.A.; Smith, M. A complete description of P- and S-wave contributions to the $B^0 \to K^+\pi^-\ell^+\ell^-$ decay. *J. High Energy Phys.* **2021**, *2021*, 85. [CrossRef]
74. Capdevila, B. Assessing lepton-flavour non-universality from $B^0 \to K^{*0}\ell^+\ell^-$ angular analyses. *J. Physics: Conf. Ser.* **2017**, *873*, 012039. [CrossRef]
75. LHCb Collaboration. Differential branching fraction and angular analysis of the decay $B^0 \to K^{*0}\mu^+\mu^-$. *J. High Energy Phys.* **2013**, *2013*, 131. [CrossRef]
76. Descotes-Genon, S.; Matias, J.; Ramon, M.; Virto, J. Implications from clean observables for the binned analysis of $B^0 \to K^{*0}\mu^+\mu^-$ at large recoil. *J. High Energy Phys.* **2013**, *2013*, 48. [CrossRef]
77. LHCb Collaboration. Measurement of form-factor-independent observables in the decay $B^0 \to K^{*0}\mu^+\mu^-$. *Phys. Rev. Lett.* **2013**, *111*, 191801. [CrossRef] [PubMed]
78. De Cian, M. Track Reconstruction Efficiency and Analysis of $B^0 \to K^{*0}\mu^+\mu^-$ at the LHCb experiment. Ph.D. Thesis, University of Zurich, Zurich, Switzerland, 2013.
79. Horgan, R.; Liu, Z.; Meinel, S.; Wingate, M. Rare B decays using lattice QCD form factors. *PoS* **2015**, *214*, 372. [CrossRef]
80. Bobeth, C.; Gorbahn, M.; Hermann, T.; Misiak, M.; Stamou, E.; Steinhauser, M. $B_{s,d} \to \ell^+\ell^-$ in the Standard Model with reduced theoretical uncertainty. *Phys. Rev. Lett.* **2014**, *112*, 101801. [CrossRef] [PubMed]
81. Beneke, M.; Bobeth, C.; Szafron, R. Power-enhanced leading-logarithmic QED corrections to $B_q \to \mu^+\mu^-$. *J. High Energy Phys.* **2019**, *2019*, 232. [CrossRef]
82. Altmannshofer, W.; Niehoff, C.; Straub, D.M. $B_s^0 \to \mu^+\mu^-$ as current and future probe of new physics. *J. High Energy Phys.* **2017**, *2017*. [CrossRef]
83. ATLAS Collaboration. Study of the rare decays of B_s^0 and B^0 mesons into muon pairs using data collected during 2015 and 2016 with the ATLAS detector. *J. High Energy Phys.* **2019**, *2019*, 98. [CrossRef]
84. CMS Collaboration. Measurement of the $B_s^0 \to \mu^+\mu^-$ decay properties and search for the $B^0 \to \mu^+\mu^-$ decay in proton-proton collisions at s=13TeV. *Phys. Lett. B* **2023**, *842*, 137955. [CrossRef]
85. LHCb Collaboration. Analysis of beutral B-meson decays into two muons. *Phys. Rev. Lett.* **2022**, *128*, 041801. [CrossRef] [PubMed]
86. Chen, K.F.; Mombächer, T.; De Sanctis, U. Analysis of $B_{(s)}^0 \to \mu^+\mu^-$ decays at the Large Hadron Collider. *Symmetry* **2024**, *16*, 251. [CrossRef]
87. Amhis, Y.; Banerjee, S.; Ben-Haim, E.; Bertholet, E.; Bernlochner, F.U.; Bona, M.; Bozek, A.; Bozzi, C.; Brodzicka, J.; Chobanova, V.; et al. Averages of b-hadron, c-hadron, and τ-lepton properties as of 2021. *Phys. Rev. D* **2023**, *107*, 052008. [CrossRef]
88. BaBar Collaboration. Search for $B^+ \to K^+\tau^+\tau^-$ at the BaBar experiment. *Phys. Rev. Lett.* **2017**, *118*, 031802. [CrossRef] [PubMed]
89. LHCb Collaboration. Search for the decays $B_s^0 \to \tau^+\tau^-$ and $B^0 \to \tau^+\tau^-$. *Phys. Rev. Lett.* **2017**, *118*, 251802. [CrossRef]
90. Belle II Collaboration. Belle II Technical Design Report. *arXiv* **2010**. [arXiv:physics.ins-det/1011.0352].
91. Choudhury, S. Lepton flavor universality at Belle and Belle II. *EPJ Web Conf.* **2023**, *282*, 01001. [CrossRef]
92. LHCb Collaboration. The LHCb upgrade I. *arXiv* **2023**. [arXiv:hep-ex/2305.10515].
93. LHCb Collaboration. Physics case for an LHCb Upgrade II - Opportunities in flavour physics, and beyond, in the HL-LHC era. *arXiv* **2018**. [arXiv:hep-ex/1808.08865]
94. LHCb Collaboration. First measurement of the differential branching fraction and *CP* asymmetry of the $B^{\pm} \to \pi^{\pm}\mu^+\mu^-$ decay. *JHEP* **2015**, *10*, 034. [CrossRef]
95. LHCb Collaboration. Evidence for the decay $B_S^0 \to \overline{K}^{*0}\mu^+\mu^-$. *JHEP* **2018**, *07*, 020. [CrossRef]
96. LHCb Collaboration. Observation of the suppressed decay $\Lambda_b^0 \to p\pi^-\mu^+\mu^-$. *JHEP* **2017**, *04*, 029. [CrossRef]
97. Belle II and Belle Collaborations. Search for rare $b \to d\ell^+\ell^-$ transitions at Belle. *arXiv* **2024**. [arXiv:hep-ex/2404.08133].
98. Kamenik, J.F.; Monteil, S.; Semkiv, A.; Silva, L.V. Lepton polarization asymmetries in rare semi-tauonic $b \to s$ exclusive decays at FCC-ee. *Eur. Phys. J. C* **2017**, *77*, 701. [CrossRef]
99. Amhis, Y.; Kenzie, M.; Reboud, M.; Wiederhold, A.R. Prospects for searches of $b \to s\nu\bar{\nu}$ decays at FCC-ee. *J. High Energy Phys.* **2024**, *2024*, 144. [CrossRef]